LASER INTERFEROMETER GRAVITATIONAL WAVE OBSERVATORY

LIGO Laboratory / LIGO Scientific Collaboration

LIGO-E080356-01-D *LIGO* 1 July 2008

HAM Crossbeam Redesign for Advanced LIGO: Technical Justification

Andy Stein, Brian Lantz, Rich Mittleman, Ken Mason

Distribution of this document:
LIGO Science Collaboration

This is an internal working note
of the LIGO Project.

California Institute of Technology
LIGO Project – MS 18-34
1200 E. California Blvd.
Pasadena, CA 91125
Phone (626) 395-2129
Fax (626) 304-9834
E-mail: info@ligo.caltech.edu

Massachusetts Institute of Technology
LIGO Project – NW22-295
185 Albany St
Cambridge, MA 02139
Phone (617) 253-4824
Fax (617) 253-7014
E-mail: info@ligo.mit.edu

LIGO Hanford Observatory
P.O. Box 1970
Mail Stop S9-02
Richland WA 99352
Phone 509-372-8106
Fax 509-372-8137

LIGO Livingston Observatory
P.O. Box 940
Livingston, LA 70754
Phone 225-686-3100
Fax 225-686-7189

Abstract
As described in previous memos (E080166 and E080328), we have developed a new design for the HAM Support Structure, to be installed in the Advanced LIGO (AdLIGO) HAM chambers. Until now, we have only made brief mention of the technical motivation for using a design that is significantly different from the Support Structure used in Initial LIGO (iLIGO). In the following discussion, we provide a more rigorous argument for making this change.

Introduction
The HAM Support Structure (D040002) mechanically couples two stages of vibration isolation. Outside the HAM vacuum chamber, four HEPI systems (D030690) provide active isolation at the four “corners” of the Support Structure. The HEPI systems are rigidly mounted to the floor via short, welded steel Piers (D020126 and D030329). Each HEPI contains one vertical and one horizontal hydraulic actuator (D030339 and D030340, respectively), which control the position of a steel interface block (D020195; referred to below as the HEPI Boot). Displacement at the output end of each actuator is measured using a differentially mounted pair of inductive position sensors. Additionally, the HEPI Boots – to which the Support Structure’s Crossbeams mount – each contain a pair of L4-C seismometers.

We use the inductive sensors to control the positions of the HEPI Boots at low frequency. This essentially locks the Support Structure to the ground at frequencies ≤ 0.1 Hz, while allowing for adjustment of the Structure’s DC position and orientation. For inertial control, we originally planned to use both feedforward from seismometers mounted to the ground and feedback from the Boot-mounted L4-Cs. Unfortunately, our ability to control using the L4-C signals is limited by some practical considerations, which are touched on below.

The Support Structure couples the four HEPI systems outside the HAM chamber (V049-4-002) to the HAM ISI system (D071400) inside the chamber. The ISI is a single-stage vibration isolation table. The bottom of the table (D071410; referred to below as ISI Stage 0) is mounted to a pair of Support Tubes (D972610), which are the in-vacuum components of the HAM Support Structure. The top of the table (D071421; referred to below as ISI Stage 1) is suspended above Stage 0, via a set of Springs and Flexures (D071430). An Optical Table (D071050) is bolted to the top of Stage 1 and provides a mounting surface for opto-mechanical components used in the LIGO interferometer. A set of six electromagnetic actuators (D071422) is mounted to the two stages, which allows us to control Stage 1’s six rigid-body degrees of freedom (DoFs). We sense motion of Stage 1 in a manner similar to that used for the HEPI system – six capacitive position sensors (D071464) measure the displacement of Stage 1 relative to Stage 0, while six GS-13 seismometers (D071470) measure the velocity of Stage 1 relative to inertial space. At frequencies ≤ 0.2 Hz (approximately), we close the loop primarily on the capacitive sensors, providing position control of Stage 1 relative to Stage 0. Above this limit – the controller’s the blend frequency – inertial feedback from the GS-13s dominates, which allows us to increase the ISI’s vibration isolation beyond what would be provided by the passive spring-mass-damper system alone. Refer to Figure 1 for the labeling conventions used for the coordinate system and for the ISI components.

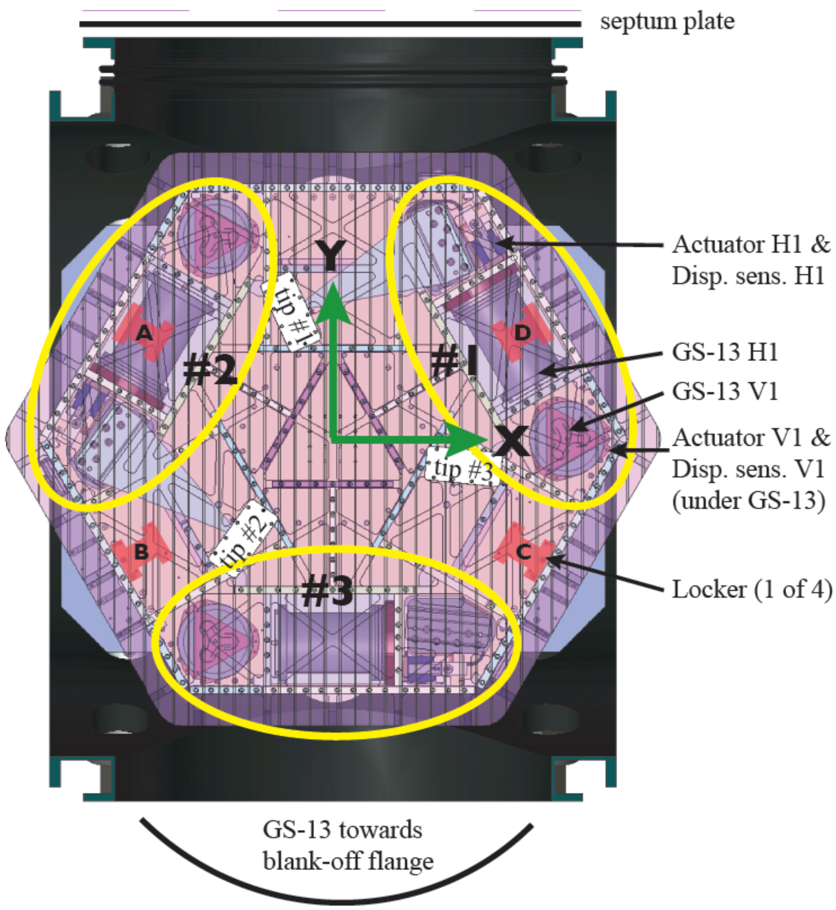

Figure 1. Top view of the ISI inside the HAM chamber. This schematic shows the relative positions of the ISI actuators, capacitive position sensors, and GS-13 seismometers. Not shown here are the Support Tubes that run underneath the ISI, parallel to the ISI's Y-axis.

With this system, we are trying to maintain Stage 1's inertia as close to constant as possible, while the motion of the ground continuously disturbs it. By comparing the motion of Stage 1 to the motion of the floor beneath it– and assuming there are no additional disturbance sources, e.g. active components mounted to the Optical Table – we can quantify the isolation performance of the combined HEPI-and-ISI system. In practice, the isolation is limited by several physical constraints. One of the key limits is the compliance of the Support Structure.

Measured Performance Data

Recently, the Seismic team installed and began commissioning two HAM ISIs – one at the LIGO Livingston Observatory (LLO) and one at the LIGO Hanford Observatory (LHO). The LHO ISI is shown in Figure 2. At both sites, the iLIGO Support Structure without HEPI (D972501) was used. We have recorded extensive performance data from the LHO ISI, which provide strong evidence that the compliance of the iLIGO Support

Structure limits the effectiveness of the HAM seismic isolation system. (At this time, we do not have a complete set of performance data for the ISI at LLO, but we expect the results there to be similar.)

Figure 2. The HAM ISI installed in its chamber at LHO.

In this analysis, we focus solely on the vertical DoF: Z-translation. The other five DoFs behave very similarly. Figure 3 shows a set of Bode plots for the LHO ISI measured after the ISI was installed in its chamber. For this data, the input signal is the drive to one of the ISI's vertical actuators, and the output signal is from the co-located vertical position sensor. As expected, the response is flat at low frequencies (< 0.7 Hz) – for a force of given amplitude applied at near-DC frequency, Stage 1 will move away from Stage 0 until the restoring force of the Springs/Flexures balances the actuation force. The displacement amplitude does not change as a function of frequency until the ISI's first rigid-body mode is excited, which occurs around 1 Hz. Based on other frequency response data taken in the coordinate basis (ie, X, Y, Z, Rx, Ry, and Rz motion of Stage 1), we know that this 1 Hz peak is a superposition of the Rx and Ry rigid-body modes of Stage 1 on Stage 0. The Z-translation rigid-body mode appears next, around 1.8 Hz.

After the two vertical rigid-body modes, we expect the displacement response to roll off as $1/f^2$, as Stage 1's inertia increasingly resists motion as the frequency (f) of excitation moves higher. If everything in the seismic isolation system were perfectly rigid, except for the ISI Springs and Flexures – and assuming those compliant members were massless – we would see the magnitude continue downward in a straight line with slope -40 dB/decade for ever-increasing frequencies. Clearly, this is not the case. Instead, we observe an anti-resonance at approximately 11 Hz, followed by a resonance at approximately 14 Hz. The resonant peak is highlighted with a black circle in the plot. At still higher frequencies, we see more anti-resonances and resonances.

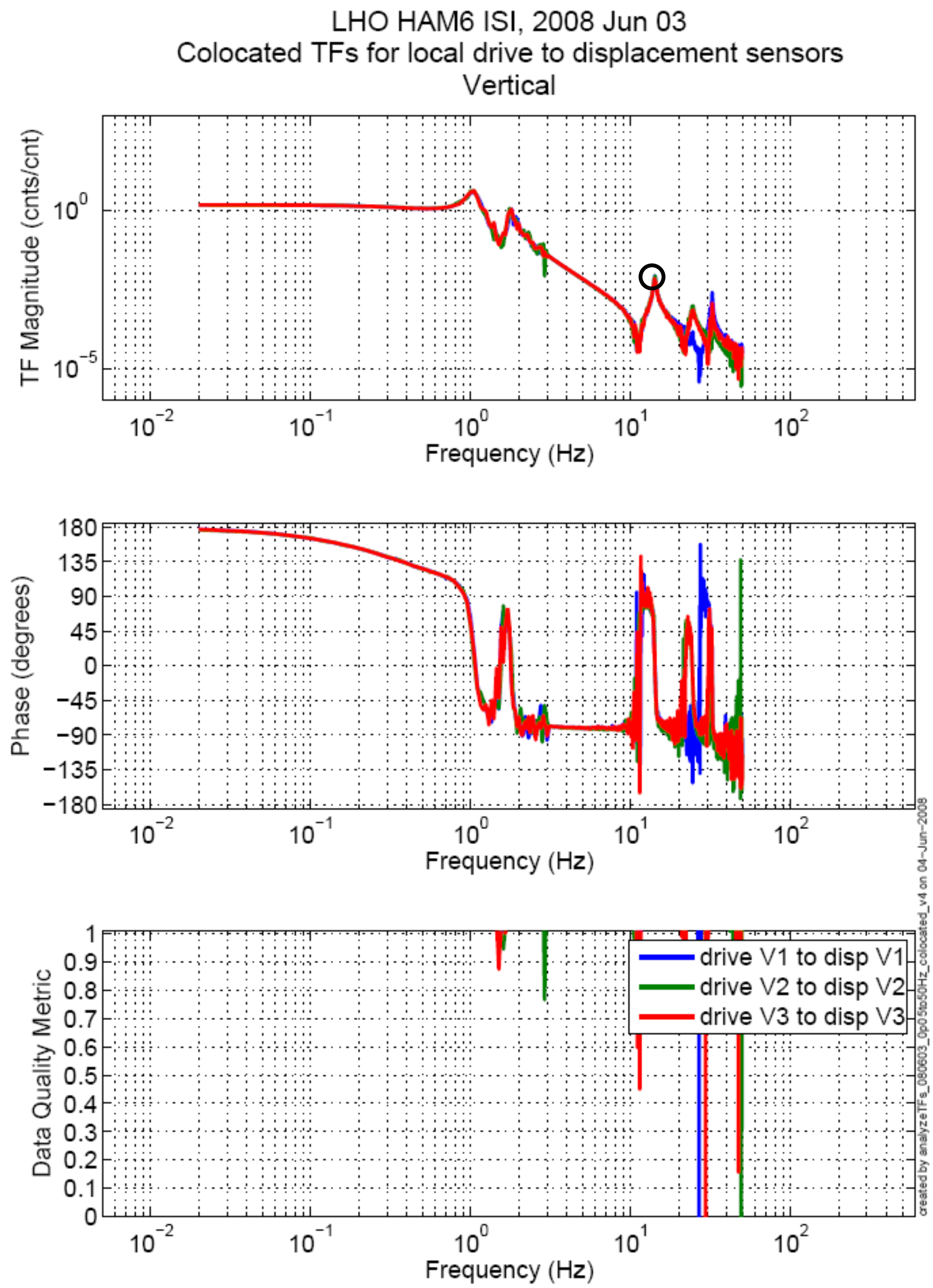

Figure 3. Local transfer functions from HAM ISI vertical actuators to Stage 1 motion, as measured by the ISI capacitive position sensors. For this data set, the ISI is mounted on an iLIGO Support Structure without HEPIs, inside the HAM chamber but at atmospheric pressure. The black circle marks the first non-rigid-body mode of the isolation system.

Now that we see evidence that the isolation system's dynamics are not "perfect", we are faced with several important questions: Can we explain what causes the additional dynamics? Do these dynamics have a negative impact on the system's isolation performance? How much improvement can we gain by directly addressing the underlying problem?

For more information, we also examine the transfer function from the ISI actuator drives to Stage 1's GS-13 inertial sensors, presented in Figure 4. This data was acquired at the same time as the displacement sensor data in Figure 3. Here, we again highlight the first non-rigid-body resonance at 14 Hz with a black circle. We see that the vertical GS-13s only register a small increase in signal at this resonance, indicating that the 14 Hz peak in the displacement sensor signal is caused primarily by the motion of Stage 0. This provides strong evidence that at 14 Hz, there is a Z-translation resonance of the Stage 0 mass on the iLIGO HAM Support Structure. Later in this report, we will provide corroborating evidence from a simple dynamic model of the system, as well as from finite element analysis (FEA) of the structure.

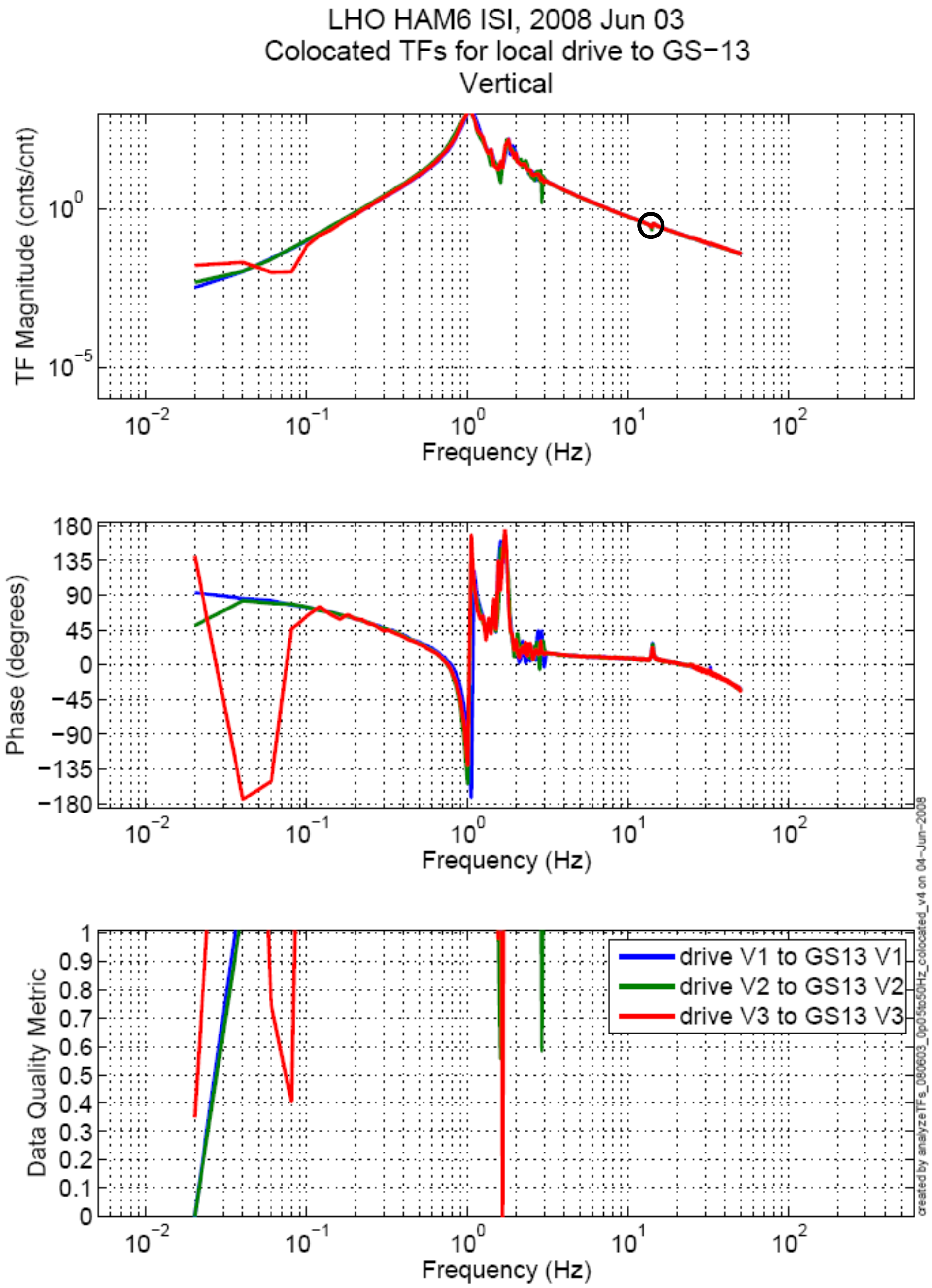

Figure 4. Local transfer functions from the HAM ISI vertical actuators to Stage 1 motion, as measured by the ISI's vertical GS-13s. We highlight the first internal mode of the Support Structure with a black circle. The mode barely registers in this inertial measurement, indicating the displacement sensor signal at this frequency is dominated by Stage 0 motion.

Quickly, we try to explain the anti-resonance in the displacement sensor data at 11 Hz. First, note that there is no change in Stage 1's inertial response at this frequency. This indicates that, at 11 Hz, Stage 0 is moving slightly on the Support Structure, roughly inphase and with the same amplitude as Stage 1. The result is a near-zero signal in the displacement sensors, even while Stage 1's inertial response is unaffected.

We see more evidence of the Stage 0 mass resonating on the compliant Support Structure at higher frequencies. At approximately 24 Hz, we see peaks in the V2 and V3 displacement sensors, with no change in the V1 response. Meanwhile, the Stage 1 inertia seems unaffected. Referring to Figure 1, we interpret this response as an Rx resonance of Stage 0 on the Support Structure, which would result in large V2 and V3 signals but small V1 signals, as the V1 sensor is located close to the X-axis. We may also attribute the next displacement peak, at 32 Hz, to an Ry resonance of Stage 0 on the Support Structure. Again, Stage 1's inertia is not affected by this mode. In this case, the V1 displacement sensor signal is larger than both the V2 and V3 signals, which also exhibit peaks at this frequency. Though it is unclear from the plot shown above, a closer look at the raw data indicates ratios of amplitudes of V1/V3 = 2.2 and V1/V2 = 10 at this frequency. It is clear from Figure 1 that the V1 displacement sensor is furthest from the Y-axis, so we expect it to have the largest signal for an Ry mode. However, we must look more carefully at the ISI assembly to note that the V2 sensor is offset toward the Y-axis, while the V3 sensor is offset away from the Y-axis. With this geometry in mind, we expect the V3 signal to be larger than the V2 signal, which is confirmed by the data. So, a brief review of the ISI plant indicates that the Support Structure's compliance introduces additional dynamics at frequencies above approximately 10 Hz.

We now compare the preceding data to similar data acquired before the ISI was installed inside the chamber. Transfer function data for the ISI mounted to the HAM ISI Test Stand (consisting of two Support Tubes mounted on four D070278 "feet" that are bolted to the floor) are shown in Figure 5 and Figure 6. Unfortunately, this data only goes up to 25 Hz, and the quality of the high-frequency displacement signal is relatively poor. With these caveats in mind, we do not see clear evidence of any dynamics other than the two vertical rigid-body modes of Stage 1 on Stage 0. This follows our expectation, since the Test Stand provides a much stiffer connection from the Support Tubes to ground, compared to the iLIGO Support Structure. (There actually is a 23 Hz mode observed in the horizontal displacement sensor data for this system. Based on FEA of the ISI on the Test Stand, we believe this mode is indeed caused by the combined compliance of the Support Tubes and the Test Stand. However, the FEA predicts the first vertical mode on the Test Stand occurs at 40 Hz, which unfortunately falls outside the frequency range shown in these plots.)

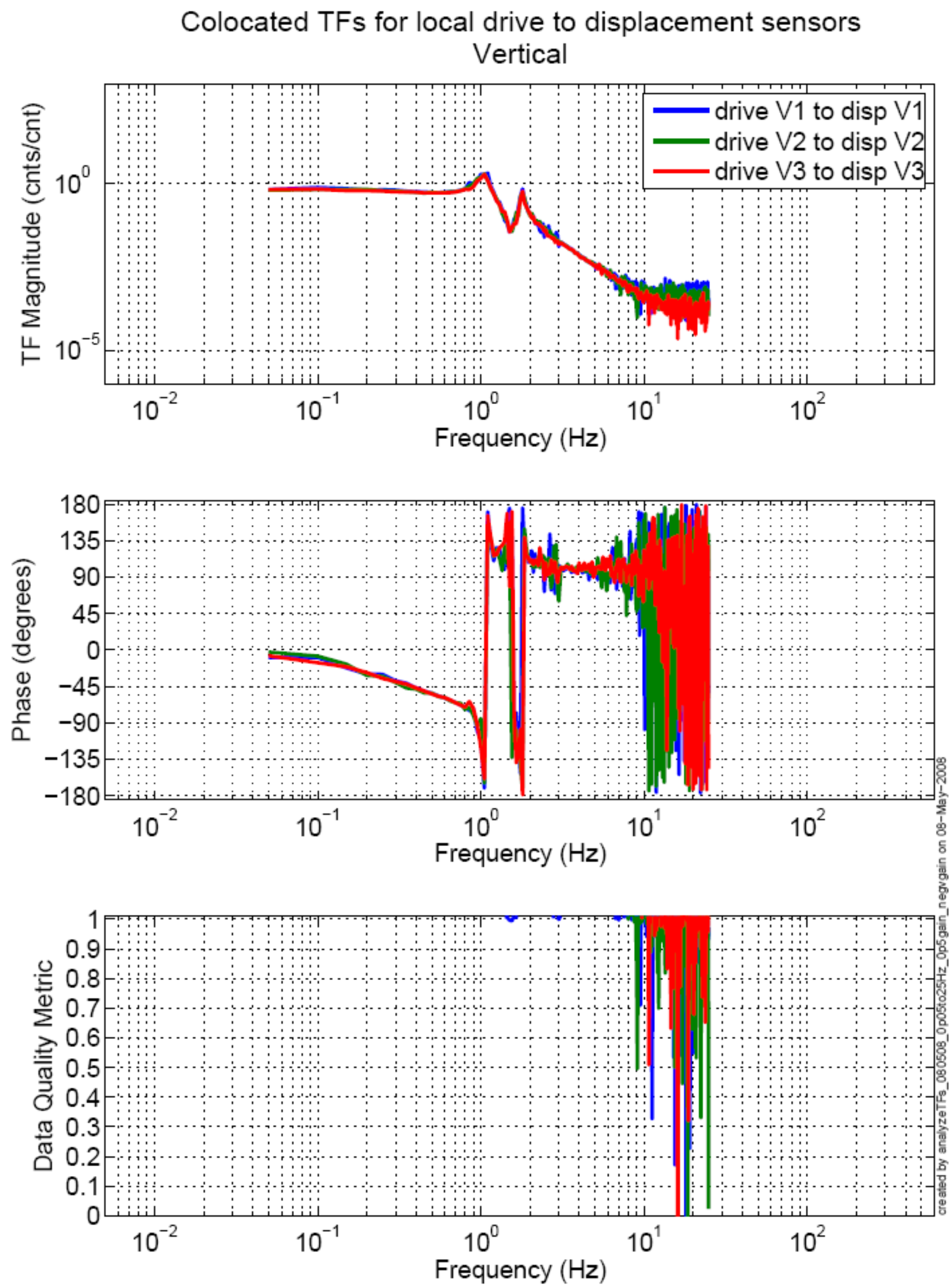

Figure 5. Co-located transfer functions for the ISI mounted to the Test Stand. For these plots, the input signal is the ISI's vertical actuator drive and the output signal is the signal from the nearest vertical displacement sensor.

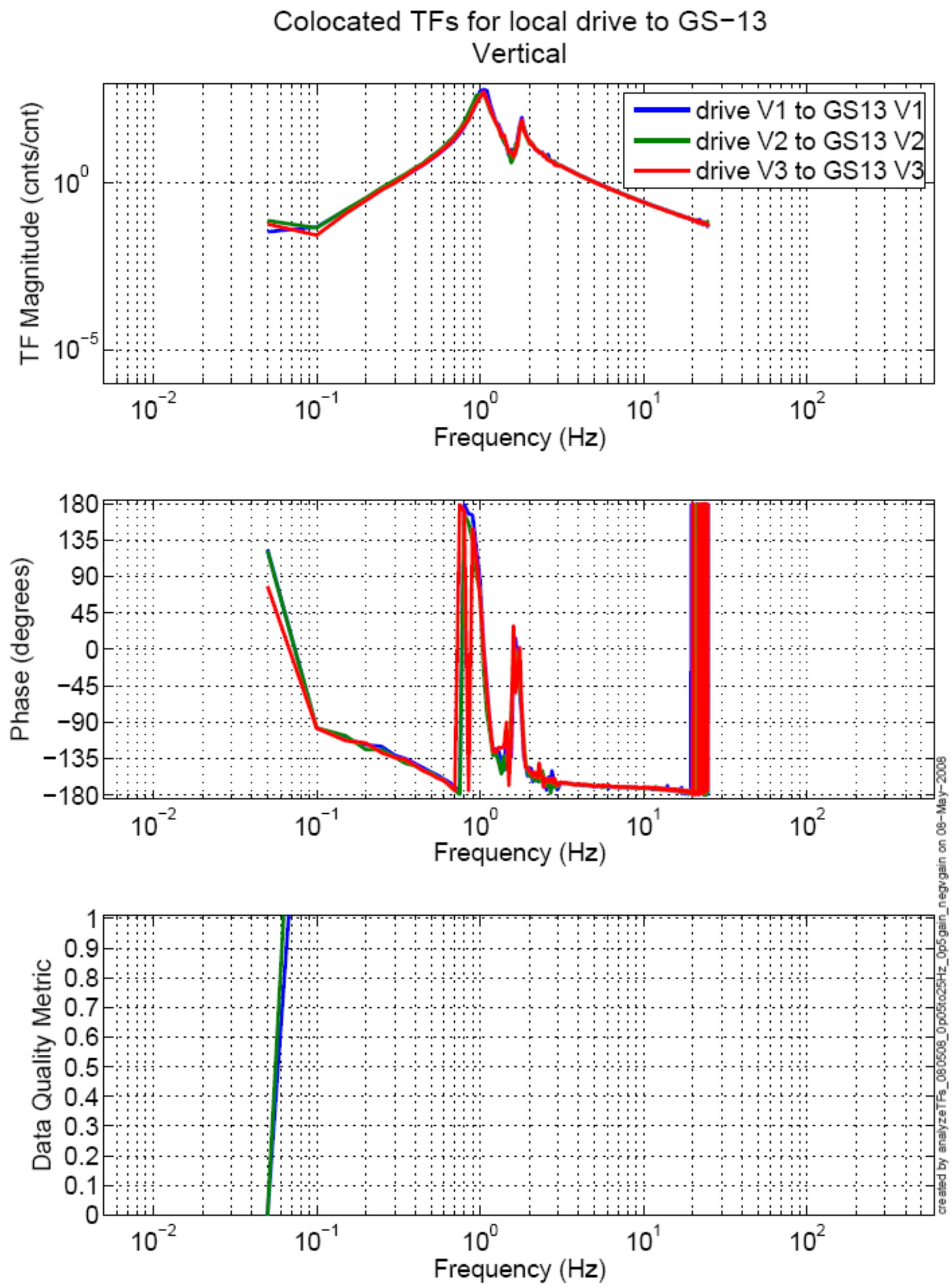

Figure 6. Transfer function data from the same measurement shown in Figure 5, but with the vertical GS-13 seismometers used as the output.

So, we have fairly strong evidence from several measurements of the ISI that the iLIGO Support Structure's compliance introduces "unmodeled" dynamics to the ISI plant. How does this effect the performance of the system after the feedback loops are closed? We have recently measured closed-loop isolation performance for the LHO HAM ISI in the HAM chamber (at vacuum pressure), which is shown in Figure 7. We see that the performance is good below the Support Structure's 14 Hz resonant frequency. At and above this resonance, the isolation performance is the same whether the system is active or passive. If we want to realize any advantage from running the system active at higher frequencies, we must increase the resonant frequencies of the Support Structure. The rest of this memo discusses how we plan to do this, and what improvement we expect to see as a result.

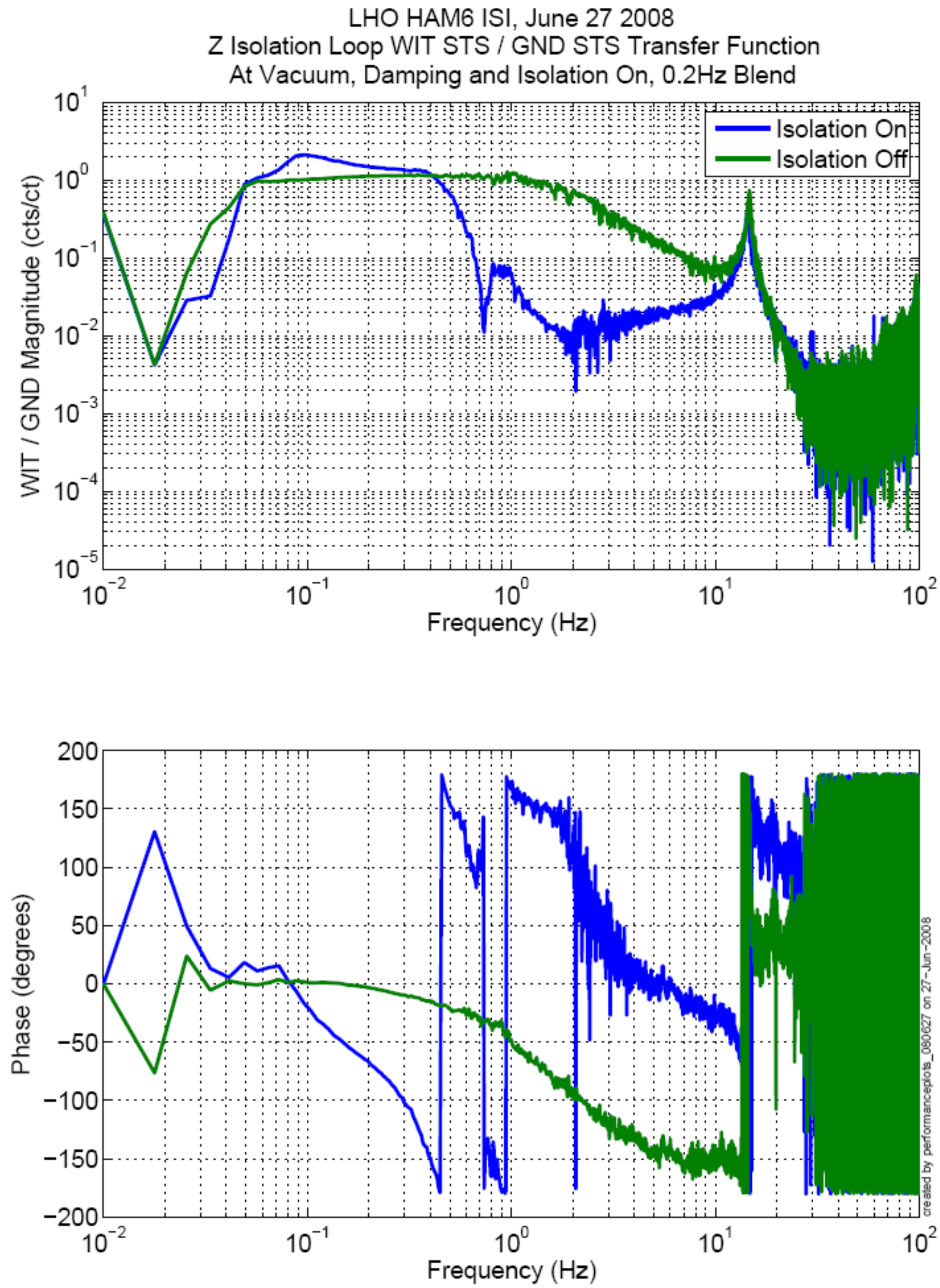

Figure 7. Bode plots for the LHO ISI in the HAM chamber, at vacuum pressure. For this measurement, the input signal is from an STS-2 seismometer resting on the ground, outside the chamber. The output signal is from an STS-2 seismometer sitting on the top of the ISI Optical Table. The difference between the “Isolation Off” and “Isolation On” curves gives an indication of how much improvement in isolation performance is gained by closing the loops on the ISI.

Modeled Performance Improvement
We have already reviewed the final design of the proposed AdLIGO Support Structure in LIGO document E080328. The CAD model is shown again in Figure 8. In that report, we present FEA results for the iLIGO Support Structure with Gullwing Crossbeams and compare them to FEA for the proposed redesign. We copy those results in Figure 9, for the predicted Z-translation mode of the two systems.

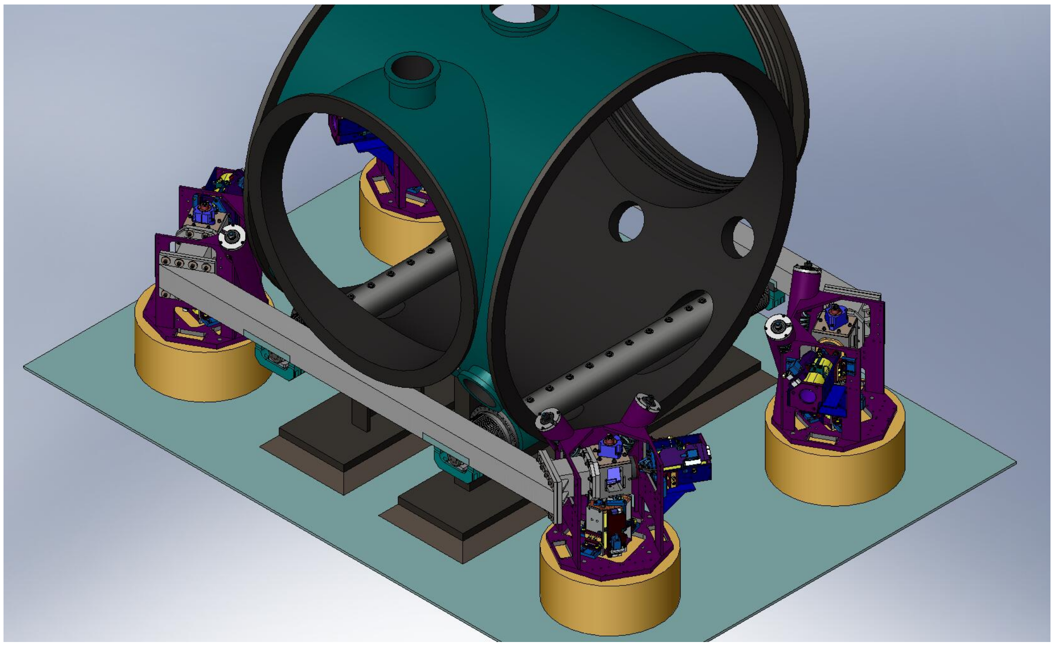

Figure 8. Screenshot of the SolidWorks model of the proposed AdLIGO Support Structure.

It is important to note two important differences between the FEA models and the physical system measured at LHO. The first item is a simplification used to make the model easier to solve: we do not include the ISI's Stage 1. Above approximately 10 Hz, the suspended mass of Stage 1 is essentially decoupled from the rest of the mechanical system. Stage 1's inertia remains close to constant, even as Stage 0 resonates on the Support Structure at higher frequencies. The stiffness of the ISI Springs (0.24 N/µm) is approximately a factor of 30x (or 70x, for the redesign) smaller than the stiffness of the Support Structure, so the presence of a quasi-fixed Stage 1 results in an insignificant restoring force to Stage 0. So, we are comfortable removing the Stage 1 model from the FEA assembly.

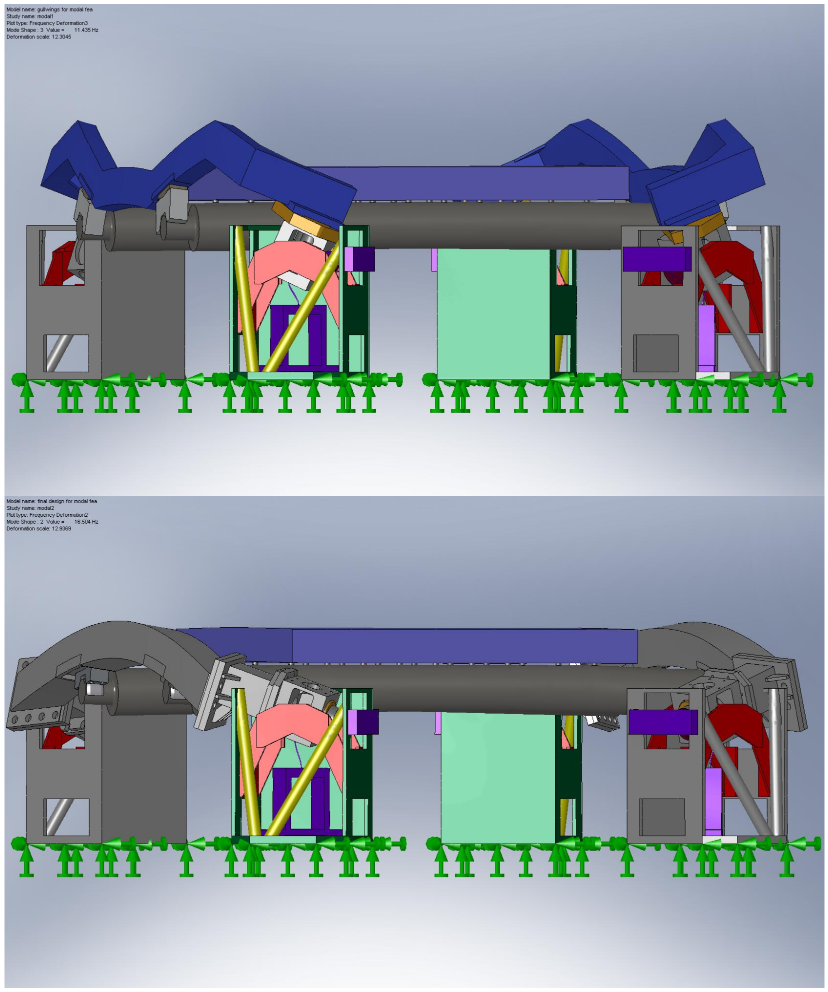

Figure 9. Mode shapes for the Z-translation resonance of ISI Stage 0 on the HAM Support Structure, for both the iLIGO Gullwing structure (top) and the proposed AdLIGO structure (bottom). The corresponding eigenfrequencies are 11.4 Hz and 16.5 Hz, respectively.

The other difference has greater impact on the analysis results. We plan to use HEPI systems at both sites for Advanced LIGO, so they are included in the FEA models. However, none of the chambers at LHO currently have HEPIs, so the data in Figure 3 and Figure 4 were taken with a significantly different mechanical system than we model here. The potential impact of this change can be inferred from the mode shapes in Figure 9. We see that the HEPI Boots, to which the Support Structure mounts, are relatively free to rotate about their connections to the HEPI actuators. (The actuators are coupled to the Boots via Tri-Pod Flexures (D020368) that are designed to be stiff axially but compliant in the other five DoFs.) This rotation reduces the effective stiffness of the system for the modes shown here. Unfortunately, we do not have an FEA model of the iLIGO Support Structure mounted as it is at LHO, so we expect the FEA to deviate somewhat from the measured system. Nonetheless, the predicted 11.4 Hz Z-translation mode for the iLIGO model still agrees fairly well with the 14 Hz mode measured on the real system.

The FEA predicts the Support Structure proposed for AdLIGO has a Z-translation resonance at 16.5 Hz, which is significantly higher in frequency than the corresponding iLIGO mode. The difference between the performance of the AdLIGO and iLIGO designs are in fact more pronounced than this. We copy over some more of the FEA results from E080328, for the iLIGO Gullwings and the AdLIGO 6"x6" Crossbeams, and present them in Table 1. As noted in that memo, we gain mostly in the horizontal stiffness of the Support Structure, since we are doubling the width of the Crossbeams, but leaving the height unchanged. We see here that the change in resonant frequencies for X and (especially) Y are greater than those for Z (on a logarithmic scale, which is the relevant scale for designing controllers).

	X **(Hz)**	***Z*** **(Hz)**	***Y*** **(Hz)**	***Rx*** **(Hz)**
Gullwing	**6.9**	**11.4**	**11.4**	**15.2**
6"x6" Crossbeam	**11.8**	**16.5**	**24.0**	**18.0**

Table 1. The first four modal frequencies predicted with FEA, for the iLIGO ("Gullwing") and AdLIGO ("6"x6" Crossbeam") Support Structures. These results are copied from E080328, which provides more details on the modeling.

Based on the FEA presented above, we are confident the proposed redesign of the HAM Support Structure will push the unwanted resonant peaks in the ISI plant to higher frequencies. Can we predict how much this will improve the seismic system's overall isolation performance?

To address this final question, we present a simplified lumped-mass model of the system (Figure 10), with three distinct masses: m_{s1} is the ISI Stage 1 mass; m_{s0}' is the "effective" modal mass of Stage 0, which includes some of the Support Structure mass; and m_{su}' is the "effective" modal mass of the Support Structure. We use "effective" masses for the Support Structure and Stage 0, since the Support Structure is really a continuous mass, with continuous stiffness (and continuous damping). Here, we only consider "fundamental" bending modes of the Support Structure, so we approximate it as a simple spring, with its mass lumped at either end – a crude approximation, but good enough for our purposes here. We couple all the masses together in series, using massless springs (with stiffness, k) and dashpots (with damping, b). The subscripts for the stiffnesses and dampings are i for the HAM Springs and Flexures, *su* for the Support Structure, and h for the HEPIs. We also include the force from the vertical ISI actuators, F_i, which is applied equally and oppositely to the masses m_{s1} and m_{s0}'.

This represents a three DoF system, with characteristic equation:

$$a_1 a_2 a_3 + a_1(b_{su}s+k_{su})m_{s0}'s^2 + (b_i s+k_i)(a_3+b_{su}s+k_{su})m_{s1}s^2 = 0,$$

where $a_1 = m_{s1}s^2 + b_i s + k_i,$
and $a_2 = m_{s0}'s^2 + b_{su}s + k_{su},$
and $a_3 = m_{su}'s^2 + b_h s+k_h.$

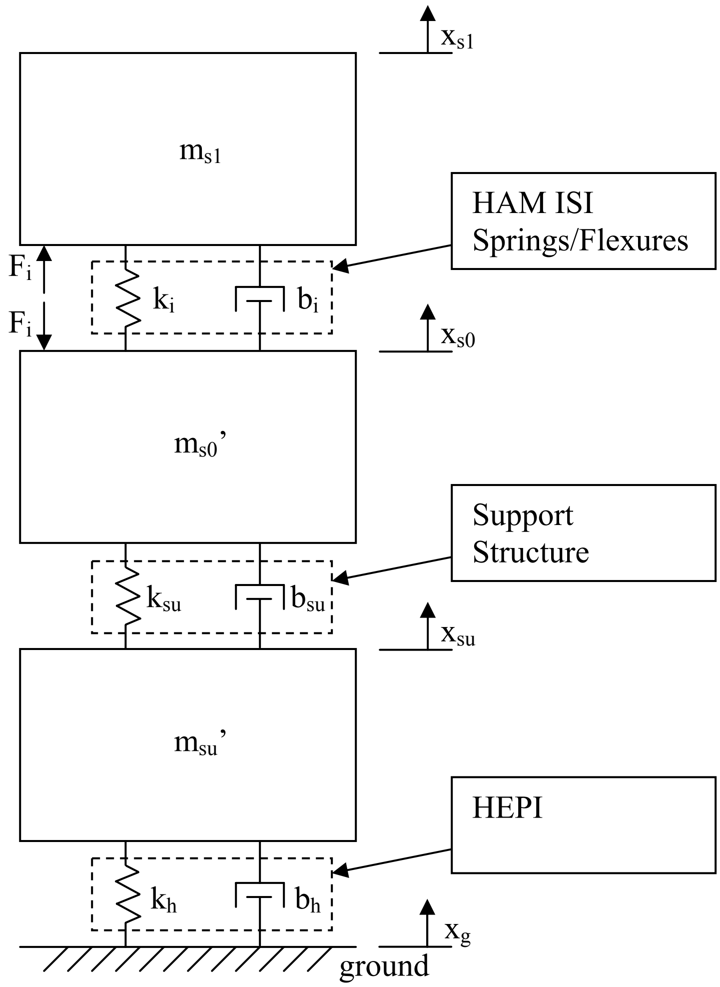

Figure 10. Lumped-mass three-DoF model of the HAM seismic isolation system.

Plugging this model into MATLAB (m-file: "three_dof_isi_rev2.m"), with representative masses and stiffnesses (and guesses for damping), we predict the transfer functions shown in Figure 11, Figure 12, and Figure 13. Note that for these transfer functions, the following assumptions apply:

1) b_{su} is the same for both designs;
2) there is no active control in either the ISI or the HEPIs;
3) there is no active damping in the ISI;
4) the vertical stiffness of HEPI is dominated by the axial stiffness of the HEPI Actuator Tri-Pods, which we have modeled as 67 N/µm per Tri-Pod;
5) there is no cross-coupling between the vertical-translation DoFs and the other DoFs;
6) we are considering the "coordinate basis" transfer functions, where only true Z-translation motion can be measured; no Rx or Ry modes are visible in this model.

The results from this model are similar both to the data acquired for the LHO ISI in the HAM chamber (Figure 3 and Figure 4) and to the FEA predictions described above. As expected, the Support Structure's resonant frequency increases when we switch to the stiffer AdLIGO design. According to our model, this mode shifts up from 12.7 Hz to 18.6 Hz. These values come close to the FEA results given in the second column of Table 1. (We should note that this logic is somewhat circular, considering the relevant parameter changed in the dynamics model – k_{su} – is taken from similar FEA studies.)

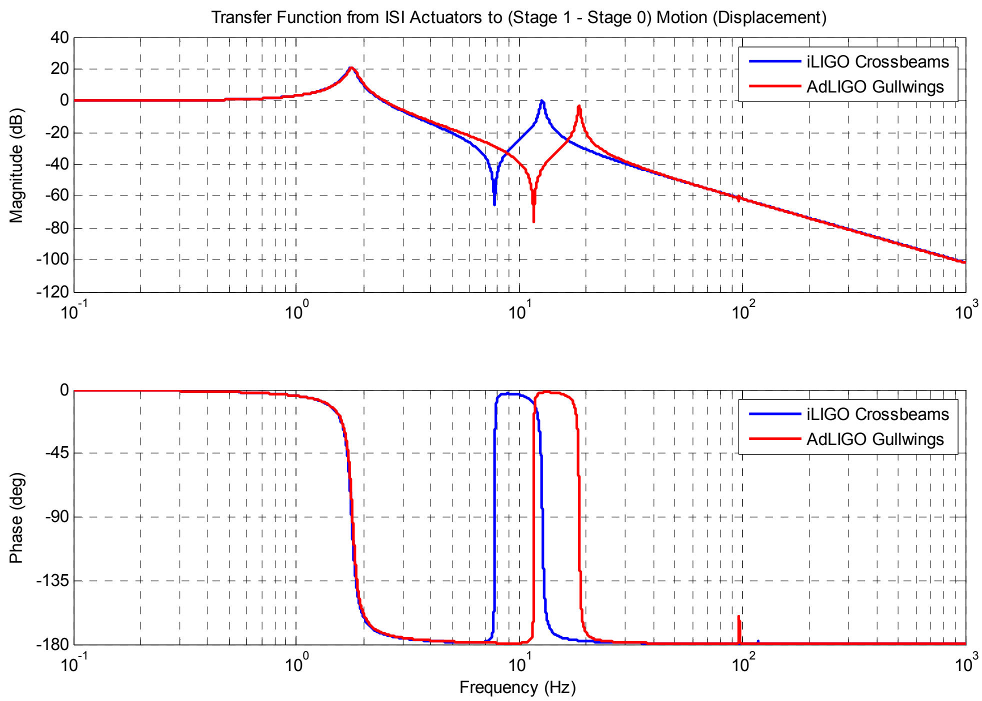

Figure 11. Predicted ISI plant transfer functions, using displacement between Stage 1 and Stage 0 as the output. These curves were generated by MATLAB and are based on the model shown in Figure 10.

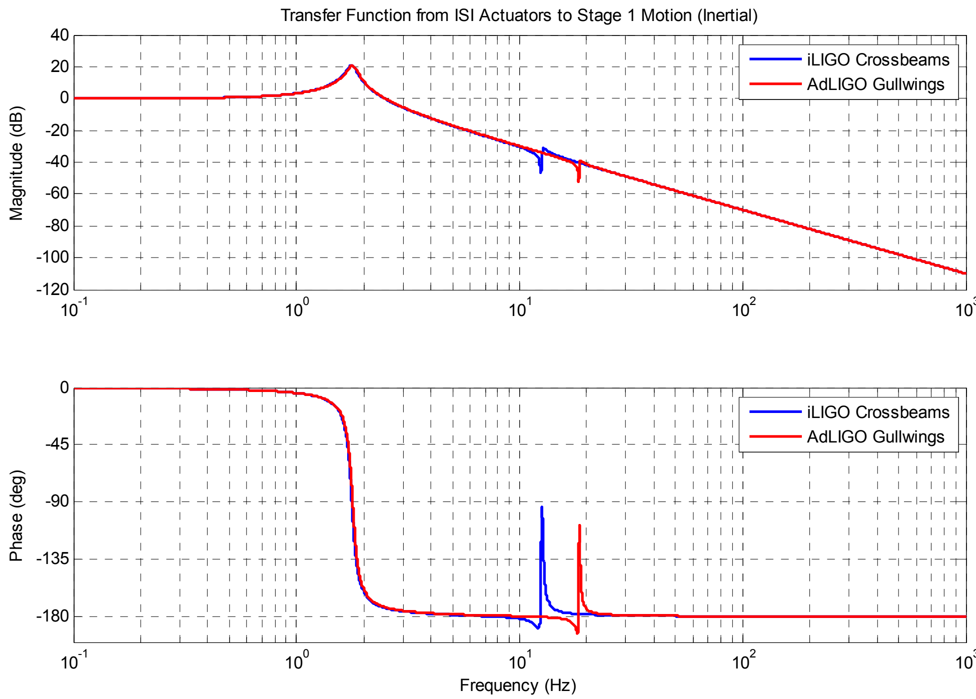

Figure 12. Predicted ISI plant transfer functions, using Stage 1's inertia as the output. Note that the low-frequency behavior is far different from the response shown in Figure 4, because we do not include the accelerometer's dynamics.

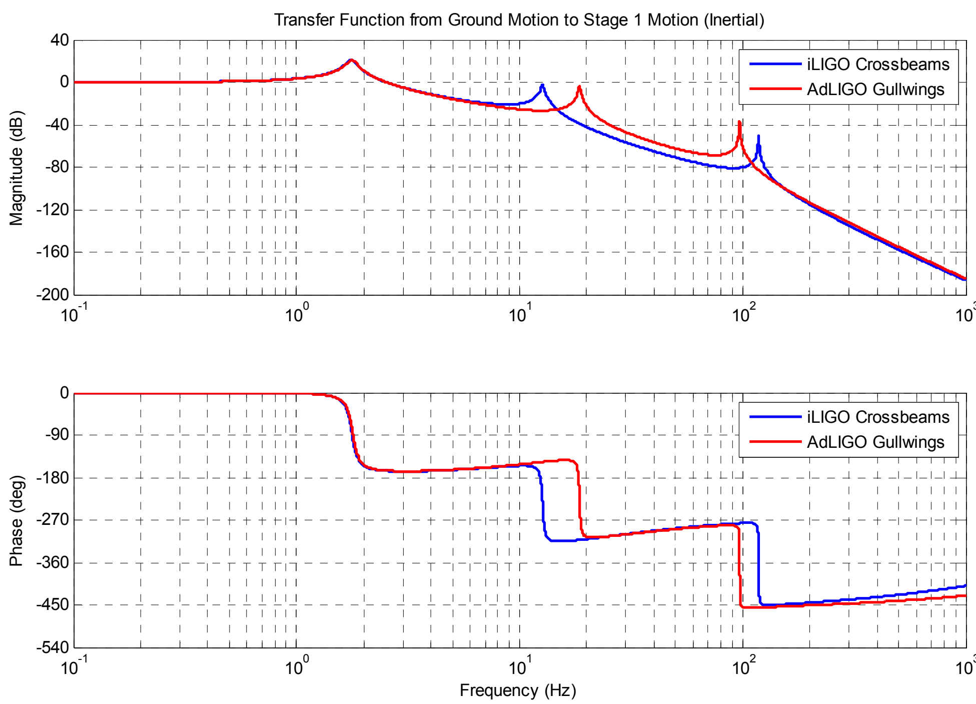

Figure 13. Predicted transfer function from ground motion to ISI Stage 1 motion, assuming only passive isolation in both the ISI and the HEPI stages.

It is interesting to note here that the proposed AdLIGO Support Structure is substantially heavier than the iLIGO Gullwing Structure – 1020 kg total, versus 700 kg (including the Support Tubes and Clamps). This results in a lower frequency for the HEPI resonance – 97 Hz, down from 118 Hz – which is shown most clearly in the response from ground motion to Stage 1 motion (Figure 13). It is also clear that both this mode and the lower-frequency Support Structure mode are strongly sensitive to the choice for distribution of the Support Structure mass. For the plots shown above, we have assumed that the mass of the Support Tubes (approximately 100 kg, each) may be lumped with the ISI Stage 0 mass. We have also assumed that an additional 50 kg from the (heavier) AdLIGO Support Structure can be lumped with Stage 0. As noted earlier, this is a crude approximation, and should be treated as such.

Conclusion

Neverthless, we have shown through both FEA and a simplified mathematical model that the "unmodeled" dynamics in the ISI plant should improve with the redesigned AdLIGO Support Structure. By pushing these resonant peaks to higher frequencies, we directly improve the isolation performance. We can imagine taking more data similar to Figure 7, where we see good isolation performance from low frequency up to the first structural mode. For that data set, the limit occurs at 14 Hz. Considering the different boundary conditions given by the HEPI systems – which we have modeled with FEA – we would expect this performance limit to occur closer to 11-12 Hz, if we continued using the iLIGO Gullwing design. With the redesign proposed for the AdLIGO Support Structure, we should instead see good performance up to approximately 16-17 Hz. In the X- and Y-translation modes, the improvement should be similar or better than this.

Though not covered in this report, we also expect better performance from the HEPI controllers, through improvement in both the Support Structure's dynamics and the tilt/horizontal coupling. Because of time constraints, we are unable to discuss these subjects in any depth. Generally, though, a stiffer structure should lead to better isolation performance.